Supplementary material

September 20, 2024

1 Fabrication of the replication master with maskless lithography

The replication master was produced at the Helmholtz nano facility (HNF). Fabrication details of the 2 step process are listed beneath.

Process step	Parameter
Dehydration	150 °C, 2 min
Spin coating	Photoresist: SU-8 2001 (Micro resist technology, Germany); 1900 rpm
Soft bake	On hot plate: 1 min at 65°C and 1 min at 95 °C
Maskless lithography	DWL66+ (Heidelberg-instruments, Germany); 13 h writing time
Post exposure bake	On hot plate: 1 min at 65°C and 1 min at 95 °C
Developer	mrDEV600 (Micro resist technology, Germany) + Isopropanol

Table 1: Process parameters for the first layer of the replication master. The layer contains the cultivation chambers and is approximately 1 µm high.

Process step	Parameter
Spin coating	Photoresist: SU-8 2010 (Micro resist technology, Germany); 2300 rpm
Soft bake	On hot plate: 3 min at 65°C and 3 min at 95 °C
Maskless lithography	DWL66+ (Heidelberg-instruments, Germany); 6 h writing time
Post exposure bake	On hot plate: 3 min at 65°C and 3 min at 95 °C
Developer	mrDEV600 (Micro resist technology, Germany) + Isopropanol

Table 2: Process parameters for the second layer of the replication master. The layer contains the supply channels and is approximately 10 µm high.

After the fabrication of the second layer the wafer was baked on a hot plate for 5 h at 150 °C.

2 Growth rate modelling

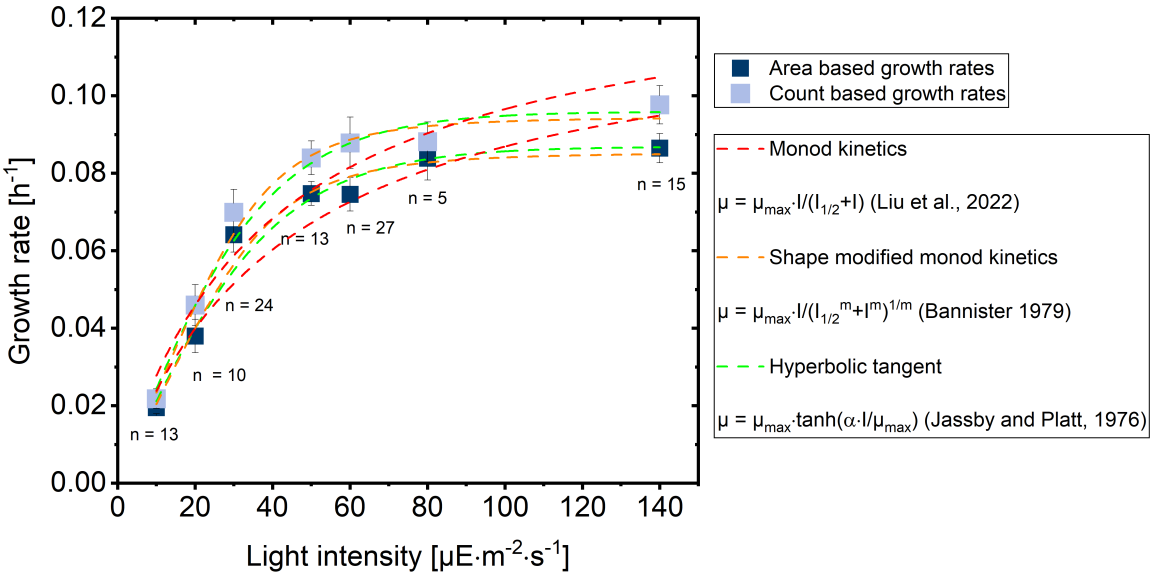

Figure 1: **Comparison of growth rate models.** *S. elongatus* UTEX2973 under homogeneous growth light illumination at 37 °C in BG11 medium. Each datapoint represents the results from a distinct growth experiment under homogeneous growth light illumination. Growth rates were calculated from fitting an exponential growth model onto the cell count (light blue) or the colony area (dark blue). Error bars indicate standard deviation. The number of evaluated chamber is indicated in the figure. Several growth models were fitted onto the data.

Growth rate model	$I_{1/2}$ [µE·m^{-2}·s^{-1}]	μ_{max} [h^{-1}]
Monod [3]	38.06	0.133
Shape modified monod [1]	40.36	0.094
Hyperbolic tangent [2]	21.14	0.096

Table 3: Model parameters from fitting three growth models onto growth rates derived from cell count

Growth rate model	$I_{1/2}$ [µE·m^{-2}·s^{-1}]	μ_{max} [h^{-1}]
Monod [3]	41.73	0.123
Shape modified monod [1]	41.73	0.085 Hyperbolic tangent [2]
22.11	0.087	

Table 4: Model parameters from fitting three growth models onto growth rates derived from cell area

The model by Jassby and Platt [2] was then chosen for fitting the growth data derived from microfluidic experiments. Fitting was performed in Origin Pro2020. The model can be seen in Equation 1.

$$\mu(I) = \mu_{max} \cdot \tanh \frac{\alpha \cdot I}{\mu_{max}} \tag{1}$$

Therein: μ_{max}: Maximum growth rate; μ: Growth rate α: Initial slope; I: Light-intensity

The maximum growth rate (μ_{max}) can be derived as follows:

$$\lim_{I\to\infty} \mu_{max} \cdot \underbrace{\tanh \frac{\alpha \cdot I}{\mu_{max}}}_{\lim_{x\to\infty} \tanh x=1} = \mu_{max} \tag{2}$$

The initial slope (α) can be derived as follows:

$$\lim_{I\to 0} \mu'(I) = \lim_{I\to 0} \mu_{max} \cdot \underbrace{\frac{1}{\cosh \frac{\alpha \cdot I}{\mu_{max}}^2}}_{\lim_{x\to 0} \cosh x=1} \cdot \frac{\alpha}{\mu_{max}} = \alpha \tag{3}$$

From the model the light-intensity at half maximum growth rate can be calculated ($I_{1/2}$):

$$\frac{\mu_{max}}{2} = \mu_{max} \cdot \tanh \frac{\alpha \cdot I_{1/2}}{\mu_{max}} \Leftrightarrow \frac{1}{2} = \tanh \frac{\alpha \cdot I_{1/2}}{\mu_{max}} \Leftrightarrow I_{1/2} = \underbrace{\tanh^{-1} 0.5}_{\approx 0.55} \cdot \frac{\mu_{max}}{\alpha} \tag{4}$$

3 Adapter between Spectra tune lab and ringlight

The Spectra Tune Lab light engine was modified to minimise the distance between the LED and ringlight, therefore maximising the intensity at the microfluidic chip. The resulting characterization of the illumination system is shown in Figure 2.

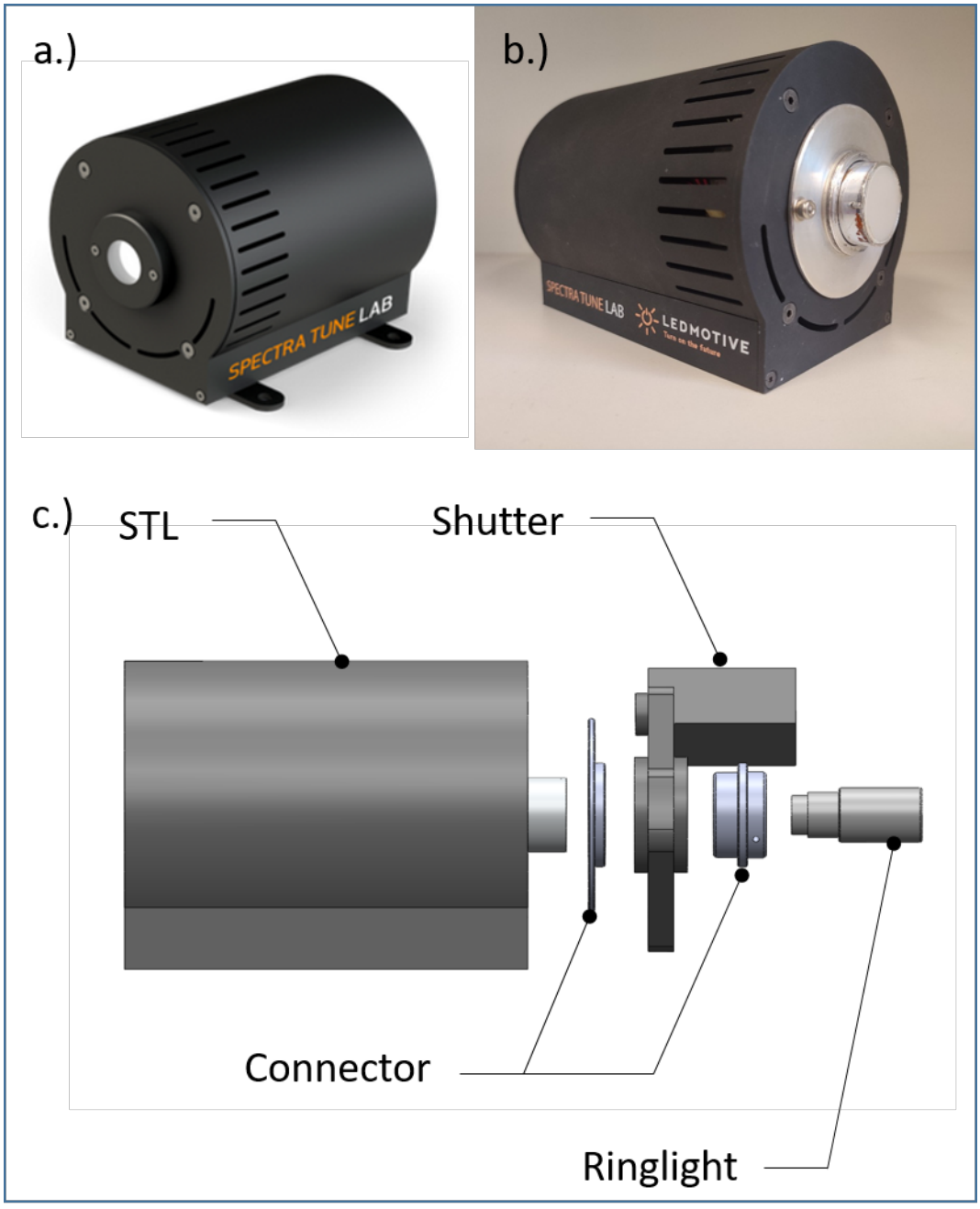

Figure 2: **Modification to the Spectra Tune Lab light engine. A.)** Original Spectra Tune Lab (STL) light engine. **B.)** The STL light engine was manipulated to yield higher light-intensities at the microfluidic chip. Therefore the distance between the inlet of the ringlight and the output of the light engine was minimized. **C.** Custom made connections between STL, shutter and ringlight

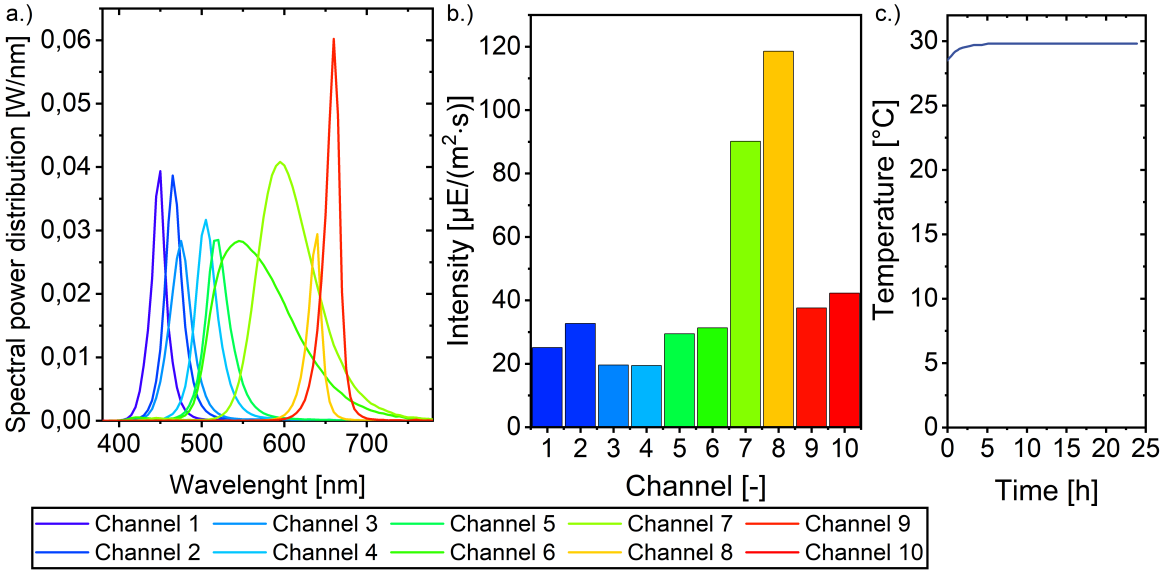

Figure 3: **Characterization of the illumination system.** The third light path was used to provide illumination to drive photosynthesis. **A.)** Spectral power distribution of the LED channels in the STL (Manufacturer information) **B.** Intensities measured with the Li190R intensity sensor at the same height at which the microfluidic chip was fixed. Power of the investigated channel was set to maximum. Intensity absorption of the microfluidic chip is negligible. **C.** The light engine was placed outside the microscope incubator to avoid interference by off-heat. To verify this, the lamp intensity was set to maximum. A temperature sensor was molded into a PDMS chip and placed at the same height as the microfluidic chip. The temperature of the sensor was monitored over 24 h. The temperature inside the incubator was set to 30 °C. No interference on temperature was observed.

4 Calibration of the light-intensity gradient

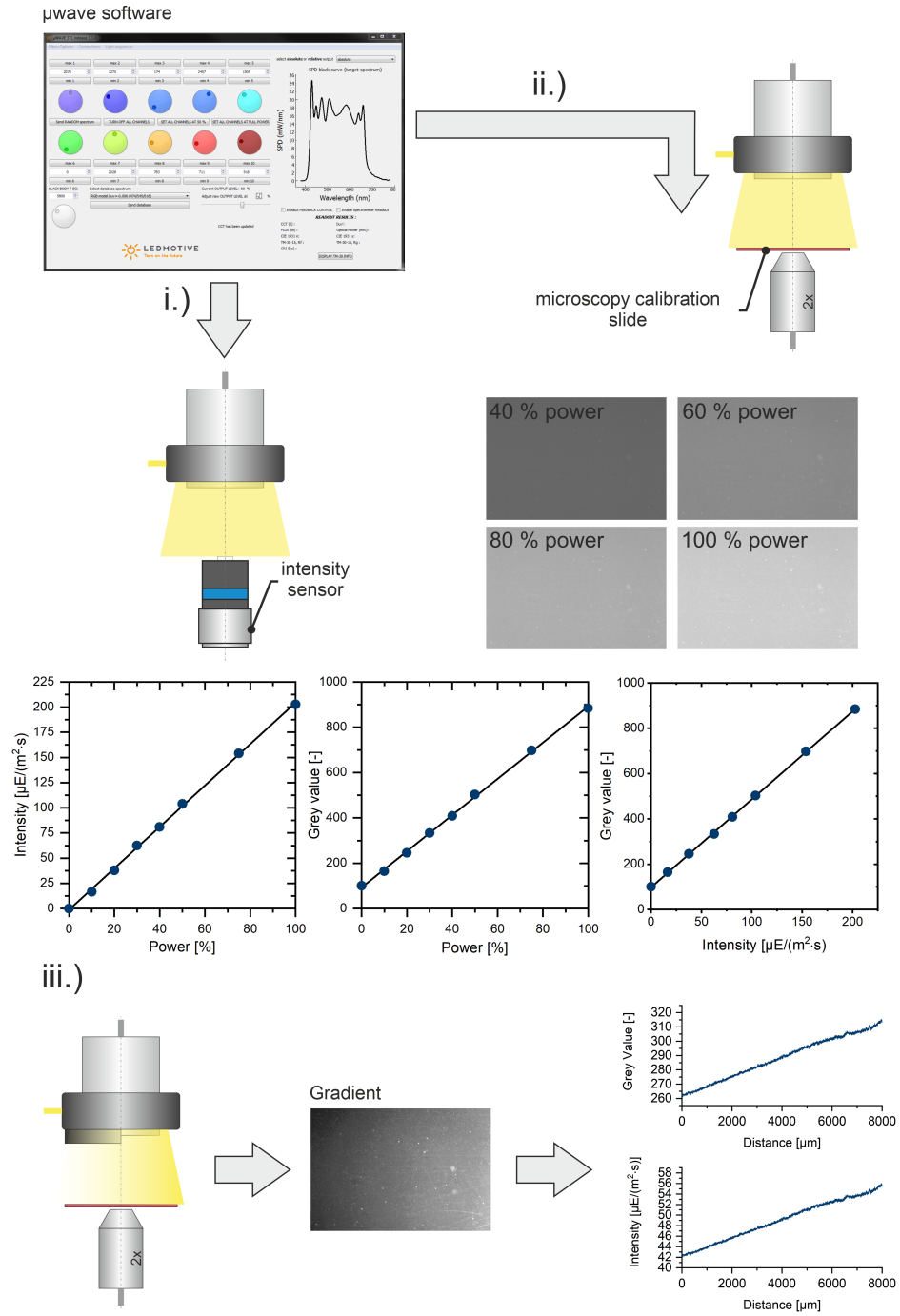

Figure 4: **Calibration of the linear light-intensity gradient.** i.) First the power setting of the light engine was correlated to light-intensity in PAR. ii.) Then the power setting of the light engine was correlated to the grey value in pictures of a microscopy calibration slide taken with a 2x objective. Here homogeneous growth light illumination was applied iii.) Then the half circle cover was installed. The resulting calibrations were used to correlate grey value to light-intensity in PAR in a picture of the microscopy calibration slide. All correlation show a $R^2 > 0.99$.

5 Light-intensity sensor

For reproducible measurements of light intensity a Li-190R intensity sensor was mounted into the microscope objective revolver. 3D CAD drawing of the connectors are supplied.

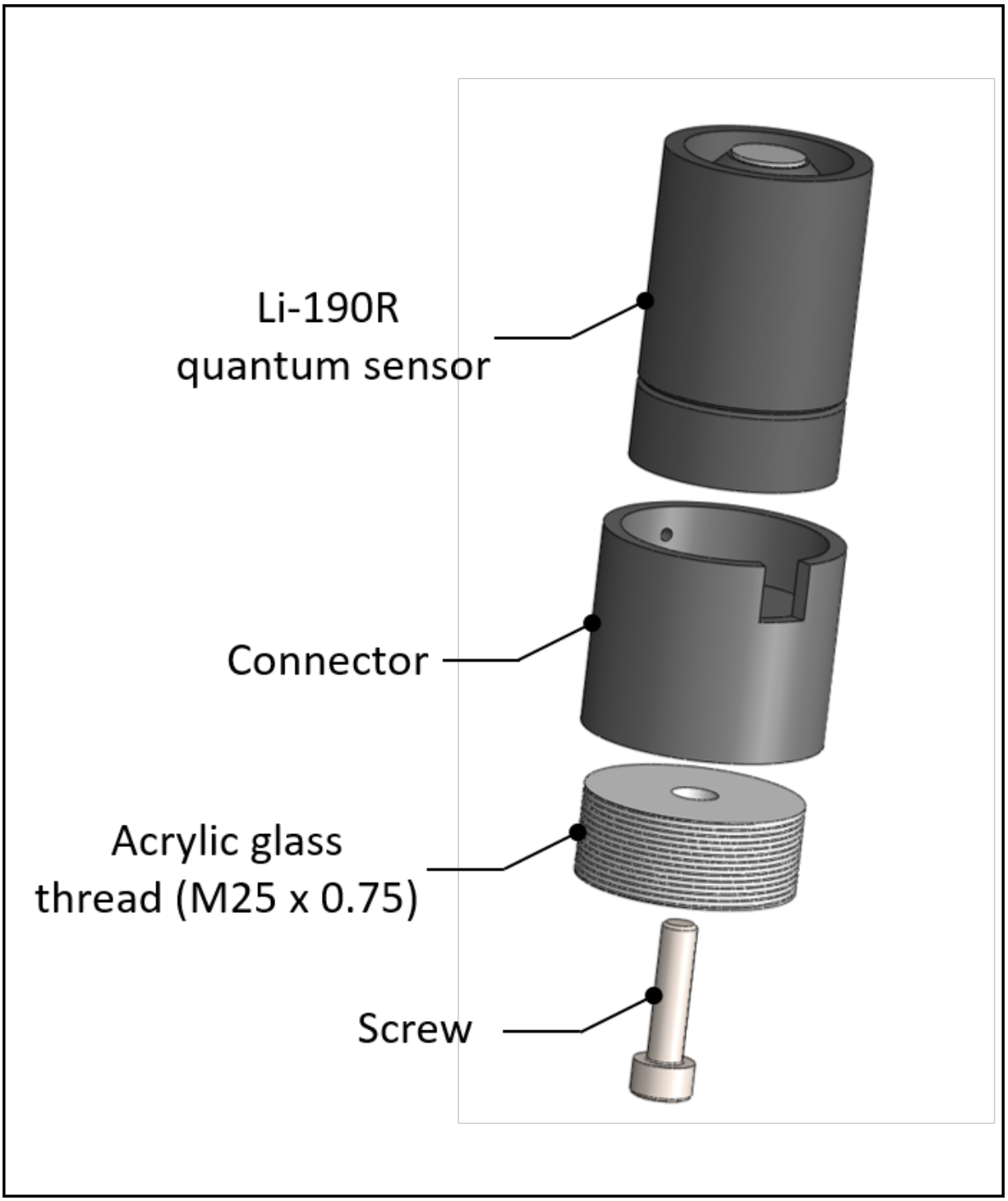

Figure 5: **Light-intensity sensor.** A Li-190R quantum sensor was used for reproducible intensity measurements. A 3D printed connector was designed to connect the sensor to a acrylic glass thread designed to fit into the objective revolver of the Ti-E. For printing a Form 3B printer equipped with Thought 2000 V1 resin was used.

6 BG11 medium

For all cultivation BG11 medium was used. All stock solution except HEPES Buffer were sterile filtrated. HEPES buffer was adjusted to pH 7 with NaOH and autoclaved. Stock solutions were mixed according to table 11 and subsequently sterile filtrated.

Component	Concentration [g/L]
$NaNO_3$	149.6
$MgSO_4$ x 7·H_2O	7.5
$CaCl_2$ x 2·H_2O	3.6
Citric acid	0.65
EDTA-Na_2	0.1

Table 5: 100 x Macronutrients

Component	Concentration [g/L]
H_3BO_3	2.86
$MnCl_2$ x 4·H_2O	1.81
$ZnSO_4$ x 7·H_2O	0.222
Na_2MoO_4 x 2·H_2O	0.391
$CuSO_4$ x 5·H_2O	0.79
$Co(NO_3)_2$ x 6·H_2O	0.4947

Table 6: 1000 x Trace metal

Component	Concentration [g/L]
K_2HPO_4	30.48

Table 7: K_2HPO_4

Component	Concentration [g/L]
Na_2CO_3	20.03

Table 8: Na_2CO_3

Component	Concentration [g/L]
Fe-NH_4-citrate	6

Table 9: Fe-NH_4-citrate

Component	Concentration [g/L]
HEPES	238.3

Table 10: HEPES Buffer

Stock solution	Concentration [g/L]
100 x Macronutrients	10
1000 x Trace metal	1
K_2HPO_4	1
Na_2CO_3	1
Fe-NH_4-citrate	1
HEPES Buffer	20

Table 11: Final composition

7 Distribution of analysed growth chambers in light-intensity gradient experiment

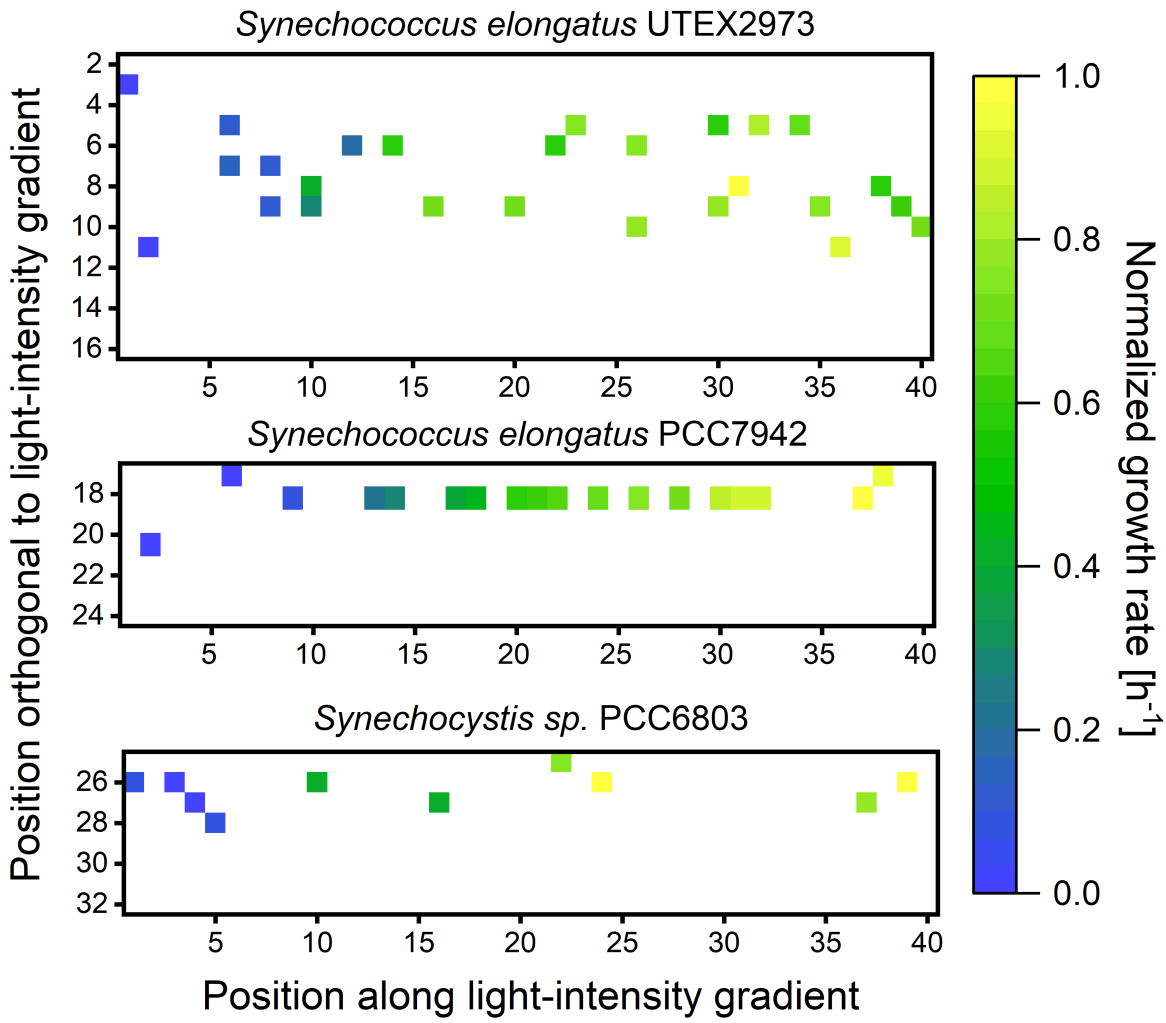

Figure 6: **Growth rate distribution within cultivation array.** The figure shows the positions of analysed chambers for the data shown in Figure 4 C. Each datapoint represents one inoculated and analysed growth chamber. The normalized growth rate is indicated by color. The light-intensity gradient is applied along the 2.4 cm long side of the chamber array. 40 chambers are distributed evenly in this direction. Each array has 8 chambers orthogonal to the light-intensity gradient. In this case *Synechococcus elongatus* UTEX2973 was inoculated in the upper two arrays. *Synechococcus elongatus* PCC7942 was inoculated beneath. *Synechocystis* sp. was inoculated in the last array. The figure shows, that there is no dependency of thrgrowth rate on the direction orthogonal to the light-intensity gradient.

8 *S. elongatus* UTEX2973 in Multi-Cultivator at various CO_2 concentrations

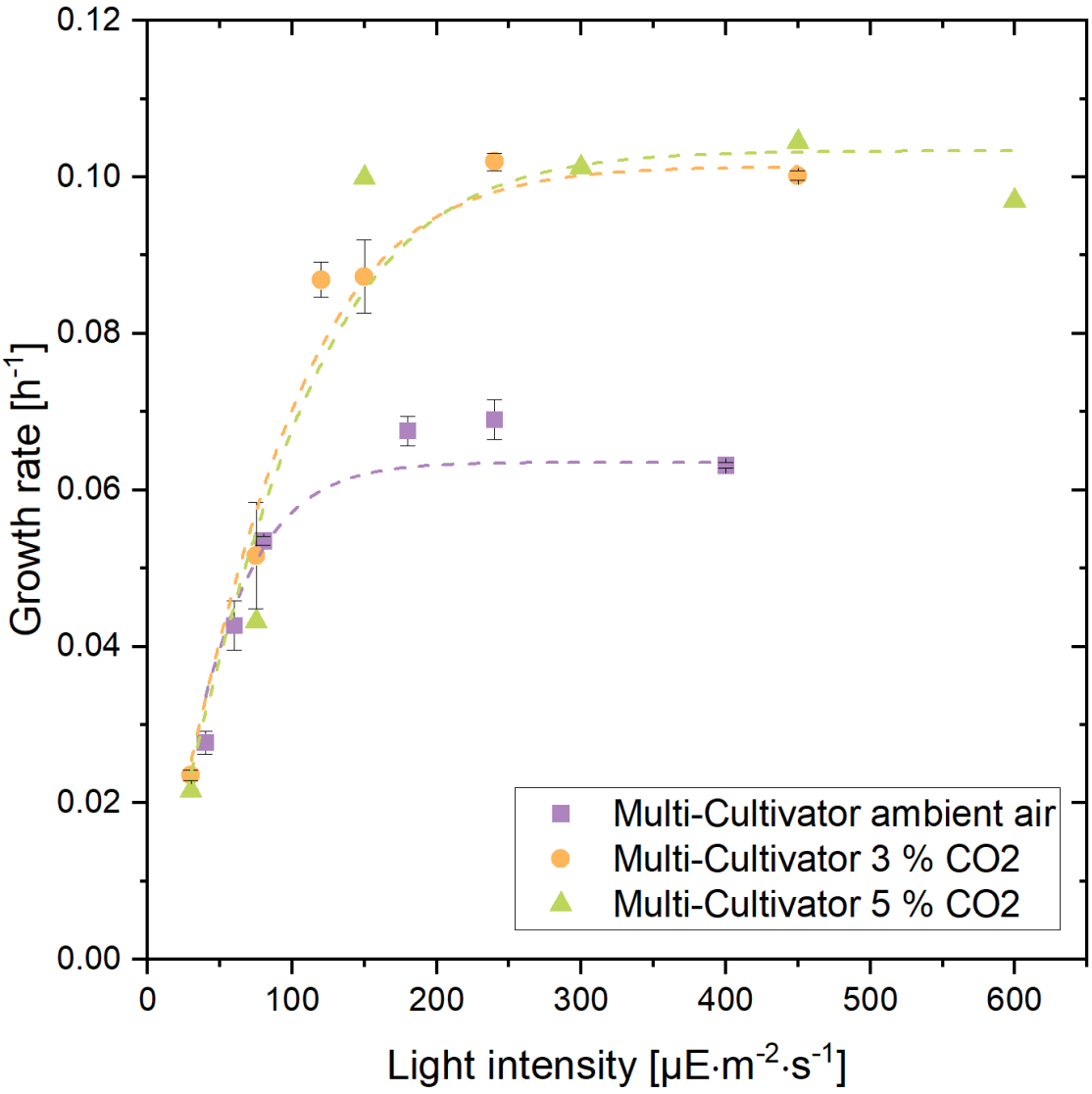

Figure 7: **S. elongatus in Multi-Cultivator with CO_2 enriched air** S. elongatus UTEX2973 was cultivated in the Multi-Cultivator at ambient air ($\approx$ 400 ppm = 0.040%), 3% and 5% CO_2. Temperature was 37 °C and BG11 medium was used. No difference between 3% and 5% CO_2 was observed indicating, that *S. elongatus* UTEX2973 grows at maximum speed when using these conditions.

9 Simulation of a simplified cultivation chip

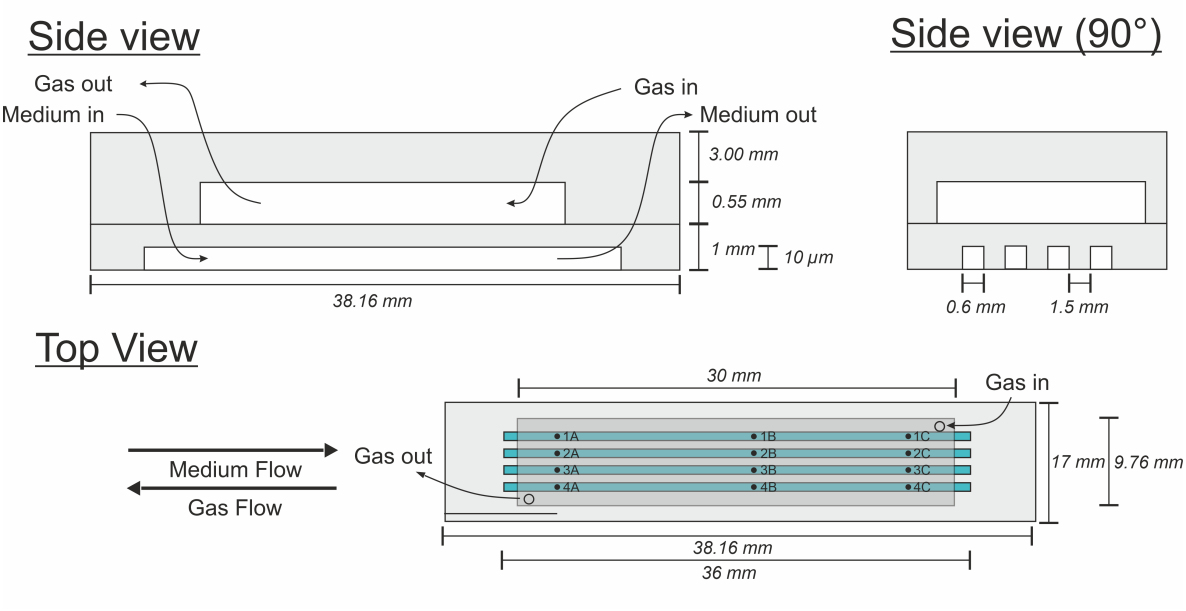

Figure 8: **Simplified model of the cultivation system.** The design of the cultivation chip was simplified to reduce complexity. First, the growth chambers were omitted, because the fluid within them is stagnant and the volume of the chambers is small compared to the volume of the supply channels. Then, the supply channels were merged into one channel with an equivalent volume, therefore keeping the velocity of the fluid constant. The gas layer was not simplified. Virtual measurement points in the COMSOL Multiphysics 6.2 simulations are indicated in the Top View.

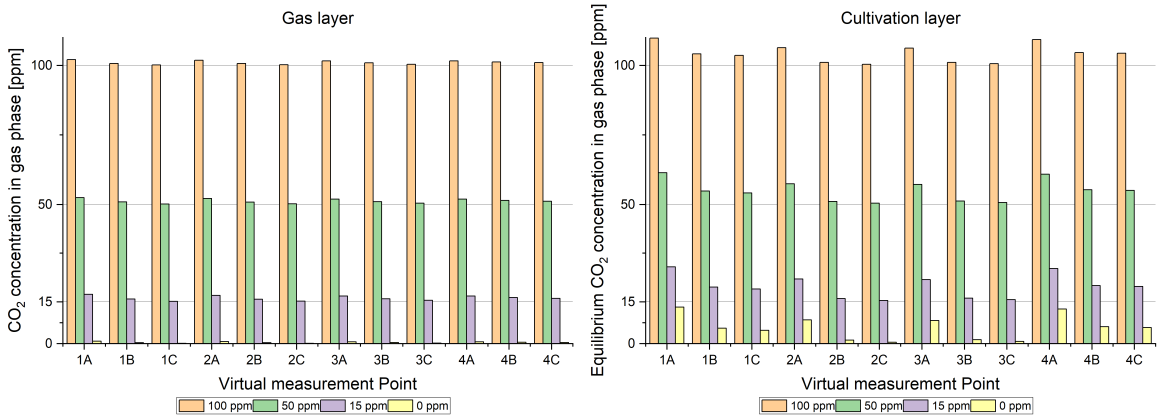

Figure 9: **Simulated CO_2 concentrations in the gas and the cultivation layers.** The CO_2 concentrations in the cultivation layer are indicated as corresponding equilibrium concentrations in the gas phase. The simulation of the CO_2 concentration in the cultivation layer has a higher inherent uncertainty for two main reasons: First, the culture layer was molded to be *as thin as possible*, so the actual thickness is less than 1 mm. Second, the cultivation layer was simplified to reduce simulation runtime.

10 Tables displaying the number of observed and analysed growth chambers

Light intensity [µE·m^{-2}·s^{-1}]	Number observed chambers	Number analyzed chambers
10	30	13
20	30	10
30	30	24
50	30	13
60	30	27
80	20	5
140	30	15

Table 12: Figure 3 F: Microfluidic cultivation under homogeneous growth-light illumination.

Strain	Number observed chambers	Number analyzed chambers
S. elongatus UTEX2973	40	33
S. elongatus PCC7942	20	18
Synechocystis sp. PCC6803	20	10

Table 13: Figure 4 C: Microfluidic cultivation of three cyanobacteria model strains under gradient growth-light illumination.

Strain	Number observed chambers	Number analyzed chambers
S. elongatus UTEX2973	40	16

Table 14: Figure 5 B: *S. elongatus* UTEX under gradient growth-light illumination with day-night rhythm.

CO_2 concentration [ppm]	Number observed chambers	Number analyzed chambers
100	30	15
50	30	19
15	30	21
0	30	15

Table 15: Figure 5 C: *S. elongatus* UTEX under gradient growth-light illumination with decreasing CO_2 concentrations. Here the growth rates were calculated for each of the 24 h periods separately. However, for some growth chambers calculation of growth rates was not possible for each CO_2 concentration.

References

[1] T. T. Bannister. Quantitative description of steady state, nutrient-saturated algal growth, including adaptation. *Limnology and Oceanography*, 24(1):76–96, 1979. _eprint: https://onlinelibrary.wiley.com/doi/pdf/10.4319/lo.1979.24.1.0076.

[2] Alan D. Jassby and Trevor Platt. Mathematical formulation of the relationship between photosynthesis and light for phytoplankton. *Limnology and Oceanography*, 21(4):540–547, 1976. _eprint: https://onlinelibrary.wiley.com/doi/pdf/10.4319/lo.1976.21.4.0540.

[3] Fangchen Liu, Larissa Gaul, Fang Shu, Daniel Vitenson, and Mingming Wu. Microscope-based light gradient generation for quantitative growth studies of photosynthetic micro-organisms. *Lab on a Chip*, 22(17):3138–3146, 2022. Publisher: Royal Society of Chemistry.